View metadata, citation and similar papers at core.ac.uk
brought to you by CORE
provided by University of Maine

The University of Maine
DigitalCommons@UMaine

University of Maine Office of Research and Sponsored Programs: Grant Reports

Special Collections

11-23-2005

ACT/SGER: Atomic Layer Deposition of Nitrides on Nano-Particles for Enhanced Energy Conversion to Combat Terrorism

William J. DeSisto
Principal Investigator; University of Maine, Orono, wdesisto@umche.maine.edu

Follow this and additional works at: https://digitalcommons.library.umaine.edu/orsp_reports

Part of the Chemical Engineering Commons

Recommended Citation
DeSisto, William J., "ACT/SGER: Atomic Layer Deposition of Nitrides on Nano-Particles for Enhanced Energy Conversion to Combat Terrorism" (2005). *University of Maine Office of Research and Sponsored Programs: Grant Reports*. 80.
https://digitalcommons.library.umaine.edu/orsp_reports/80

This Open-Access Report is brought to you for free and open access by DigitalCommons@UMaine. It has been accepted for inclusion in University of Maine Office of Research and Sponsored Programs: Grant Reports by an authorized administrator of DigitalCommons@UMaine. For more information, please contact um.library.technical.services@maine.edu.

Final Report for Period: 09/2003 - 08/2005 **Submitted on:** 11/23/2005
Principal Investigator: DeSisto, William J. **Award ID:** 0346124
Organization: University of Maine
Submitted By:

Title:
ACT/SGER: Atomic Layer Deposition of Nitrides on Nano-Particles for Enhanced Energy Conversion to Combat Terrorism

Project Participants

Senior Personnel

Name: DeSisto, William
Worked for more than 160 Hours: Yes
Contribution to Project:

Post-doc

Graduate Student

Undergraduate Student

Technician, Programmer

Other Participant

Research Experience for Undergraduates

Organizational Partners

Yardney/Lithion Inc.
Coin cell batteries were prepared and characterized at Yarndey/Lithion.

Other Collaborators or Contacts

Activities and Findings

Research and Education Activities:
We investigated the use of a conducting titanium nitride TiN coating on nanoparticles for passivating the surface and enabling higher surface area material for use in lithium-ion batteries. The TiN coatings were prepared by atomic layer deposition (ALD). Coatings were formed on silica powder, lithium titanate spinel and silicon, the latter two anode material for lithium-ion batteries. The project was broken down into two phases: (i) obtain a fundamental understanding of the atomic layer deposition (ALD) of TiN on nanoparticles and (ii) evaluate the effect of the TiN coating on lithium battery performance.

Educationally, this research has contributed significantly to a Ph.D. student's thesis. The student gained experience in interacting with a small business (Yardney/Lithion). This work has strengthened collaboration between the University of Maine and Yardney/Lithion.

Findings: (See PDF version submitted by PI at the end of the report)

Training and Development:

The Ph.D. student received research skills in materials synthesis and characterization. The student also received teaching skills by preparing and delivering a class lecture (senior university level) on his research experience.

Outreach Activities:

A gifted female high school student (junior) spent 6 weeks during the summer at the University of Maine spending time experiencing a wide breadth of materials chemistry-related research including this research topic. We have plans for her to present her experience to her high school classmates and teachers this fall. We hope this starts a fruitful relationship between high school students and University of Maine research.

Journal Publications

Books or Other One-time Publications

Web/Internet Site

Other Specific Products

Contributions

Contributions within Discipline:

Titanium nitride is a refractory material that conducts electricity well. It has found many uses as a thin layer in microelectronics processing. Methods to deposit TiN thin films include atomic layer deposition (ALD). ALD is achieved by the sequential two-step reaction of titanium tetrachloride (responsible for depositing titanium) and ammonia (nitrogen source). In this manner, atomic level control of the film growth is achieved. For ALD of TiN on silica surfaces observed growth rates are much lower than expected. As part of this project, we have taken the time to investigate possible causes for this. Through careful experimental work we have observed that during the initial stages of film deposition the ammonia actually cleaves some of the titianium chloride surface species from the silica surface. In addition, some existing TiN is converted to titanium oxide. These reaction processes limit the overall growth rate of TiN via ALD.

A particular goal of this project was to investigate materials that could increase the amount of energy that can be packed into a lithium ion battery. One way to do this is to use nanoparticles. Chemical reactions that generate electricity take place on the surfaces of tiny particles. By making these particles smaller, the amount of energy stored and generated can be increased per unit volume. However, chemical reactions on nanoparticles tend to occur too quickly. We investigated the use of TiN as a layer on the surface of nanoparticles to better control these chemical reactions. The synthesis of such layers on nanoparticles is a significant challenge. Research contributed to fundamental understanding of the relationship between preparation conditions and material properties. One particular challenge we discovered was during nanoparticle coating it was difficult to keep the nanoparticles from agglomerating into larger particles. Research also demonstrated that TiN coatings on electrode material allowed the formation of a reversible battery. These preliminary results were encouraging in that further exploration of these ideas might lead to lithium ion battery improvements.

Results generated in this project will impact the nanoscience community and the energy conversion community.

Contributions to Other Disciplines:

Contributions to Human Resource Development:

This project has contributed to the Ph.D. education of one student. It has also contributed to development of a science technician. It has contributed to the growth and development of a talented female high school junior who is interested in pursuing a career in science.

Contributions to Resources for Research and Education:

This project has provided information resources for chemical engineering undergraduate curriculum at the University of Maine. Examples from research results have been incorporated into two classrooms, an upper class technical elective and a first year engineering class, both taught by the PI.

Contributions Beyond Science and Engineering:

Conference Proceedings

Categories for which nothing is reported:

Any Journal
Any Book
Any Web/Internet Site
Any Product
Contributions: To Any Other Disciplines
Contributions: To Any Beyond Science and Engineering
Any Conference

NSF Final Report

Project Number: CHE-0346124

Project Title: Atomic Layer Deposition of Nitrides on Nano-Particles for Enhanced Energy Conversion to Combat Terrorism

Funding Period: 9/1/03-9/1/05
Funding Level: $84,767

Prepared by: William J. DeSisto

Summary of Results

The objective of this project was to provide novel nano-materials for greatly increasing energy conversion in lithium batteries. It was a collaborative project with Yardney Technical Products, Inc/Lithion, Inc. The use of nano-materials in high energy lithium batteries has been limited because of uncontrolled surface reactions between the electrolyte, solvent, and the high surface area electrode material. We investigated the use of a conducting titanium nitride TiN coating on nanoparticles for passivating the surface and enabling higher surface area material for use in lithium batteries. The TiN coatings were prepared by atomic layer deposition (ALD). The project was broken down into two phases: (i) obtain a fundamental understanding of the atomic layer deposition (ALD) of TiN on nanoparticles and (ii) evaluate the effect of the TiN coating on lithium battery performance.

The synthesis and characterization of TiN layers on nanoparticles via ALD has led to interesting results regarding the formation mechanism, particularly in the early stages of layer formation, which is critical when coating a nanoparticle because ultimately the coating layer should be thin. Our technique involved the sequential deposition of two surface limited half reactions leading to one theoretical monolayer of TiN. The two half reactions were: (A) $TiCl_4$ reacting with the N-H terminated surface and (B) NH_3 reacting with the Ti-Cl terminated surface. Between half-reactions A and B, excess reactant was purged from the system with inert gas. Repeated AB cycling of these half-reactions led to the formation of TiN layers. These sequenced reactions occurring on silica were examined in-situ via FTIR spectroscopy. Ex-situ characterization included Raman spectroscopy, DRIFT IR spectroscopy, X-ray photoelectron spectroscopy and X-ray diffraction.

A reaction mechanism was elucidated for TiN formation from $TiCl_4$ and NH_3 on silica. These results were presented at the 2004 NSF Approaches to Combat Terrorism Workshop and submitted to *Thin Solid Films* as a manuscript. In the initial half-reaction of $TiCl_4$ on silica all hydroxyl modes are reacted. Upon exposure to ammonia, some TiN is formed along with a regeneration of silicon hydroxyls, as observed by FTIR. As layers progress, some TiN is oxidized to TiO_2 also. As a result, there are two separate competitive reactions going on: (i) TiN formation and silica regeneration and (ii) TiN formation and TiO_2 formation. It is assumed that the presence of small amounts of water vapor contribute to both competitions, particularly the second one. It is not clear yet what role ammonia plays in the first competition. It takes approximately 50-100 reaction cycles to achieve a stable TiN layer as observed by Raman spectroscopy. This corresponds to an approximate layer thickness of 30Å (based on literature values).

Thin films of TiN were formed on both $Li_4Ti_5O_{12}$ and Si nanoparticles. The reaction rates for TiN on these materials were considerably higher than on silica due to the differences in surface chemistry. A series of depositions were performed varying cycle time and growth temperature. The coatings were analyzed for nitrogen content and morphology using analytical techniques. Coated $Li_4Ti_5O_{12}$ samples were used to fabricate coin cells at Yardney Technical Products, Inc./Lithion, Inc. and compared to non-coated $Li_4Ti_5O_{12}$ samples. A reduction in capacity for the coin cells from 145 to 30 mAh/g was measured for the TiN-coated anodes. It was concluded that the TiN-coated samples could work as a reversible anode in a lithium-ion coin cell, however further optimization of the coating process as well as the battery fabrication methods need to be examined to draw firmer conclusions.

We expect this work will result in two refereed journal articles and contribute significantly to a Ph.D. student's thesis. The student gained experience in interacting with a small business (Yardney/Lithion). This work has strengthened collaboration between the University of Maine and Yardney/Lithion.

The results of this report are divided into three sections. The first section, “An Infrared Study of the Surface Chemistry of Titanium Nitride Atomic Layer Deposition on Silica from $TiCl_4$ and NH_3,” details the study of the formation of the TiN thin film on fumed silica. The second section, “Synthesis and Characterization of TiN Thin Film Coatings on Si and $Li_4Ti_5O_{12}$ Nanoparticles**,”** concentrates on the formation of bulk thin films on Si powder and $Li_4Ti_5O_{12}$ powders. The final section is entitled “Performance of TiN-Coated $Li_4Ti_5O_{12}$ Powder in a Lithium-Ion Battery” and concerns the lithium-ion battery testing conducted by Yardney/Lithion. All sections include an introduction, description of experimental method, results and conclusion.

An Infrared Study of the Surface Chemistry of Titanium Nitride Atomic Layer Deposition on Silica from $TiCl_4$ and NH_3

1. Introduction

Titanium nitride (TiN) is a conducting, refractory material that has been researched for a variety of thin film applications. TiN thin films have been widely used as diffusion barriers for metal interconnects in ULSI processing [1-4], cutting tools, solar films for windows, and even for decorative purposes [5-7]. Traditionally, physical vapor deposition techniques have been used to synthesize TiN thin films. Though they are useful because of their low reaction temperatures, they offer poor step coverage [3, 5]. Chemical vapor deposition (CVD) is often used to produce more conformal films for surfaces with features such as trenches [1, 3, 8, 9].

Atomic layer deposition (ALD) is an attractive method for synthesizing thin films. Conformality and step coverage of ALD films is much greater than those created by other deposition methods [5, 10-12]. In ALD, film deposition is achieved by repeated cycling of half-reactions (for a binary film) of individual precursors. These gaseous precursors are introduced individually followed by an inert gas purge of the reactor system. Each of the precursors saturates the substrate surface, thus allowing control of the thickness of the deposited film [5, 13, 14]. Ritala used $TiCl_4$ and NH_3 and introduced a reducing zinc pulse in between the two precursors to deposit a film on soda lime glass. The zinc led to a change in the appearance of the film and its electrical resistivity [5]. Kim *et al.* used $TiCl_4$ and NH_3 on p-type Si wafers (1 0 0) [13], while Lim *et al.* used tetrakis-dimethylamino titanium (TDMAT) and NH_3 on Si (1 0 0) to allow lower reaction temperatures (60-240ºC) and eliminate chlorine contamination and corrosion [14, 15]. Min *et al.* used tetrakis(ethylmethylamino) titanium (TEMAT) and NH_3, also at lower reaction temperatures than those required for $TiCl_4$ [16] .

Applications requiring a high surface area with specific surface properties may be realized by coating particles by ALD. To this point, a modest amount of work has been done recently regarding ALD on powders [17-20]. ALD on high surface area materials has been described by Lindblad [21] and Huakka [22] and is preceded by the work of Aleskovskii *et al.* [23-25] plus numerous other examples cited by Puurunen [26]. BN particles have been modified with coatings of SiO_2 [27, 28] and Al_2O_3 [29], and coatings of TiO_2 have been formed on SiO_2 [30, 31] and kaolin [31]. But, in general, most ALD work has been performed on traditional planar substrates with minimal focus on powder substrates. We are interested in using ALD to generate TiN coatings on high surface area particles. The high conductivity of TiN makes it an attractive candidate for passivating the surface of smaller electrode particles and thus could lead to the use of higher surface area electrode material in high-energy lithium-ion batteries.

Clearly, it is important to understand the fundamental surface chemistry in the ALD process and its relationship to film properties. In an ALD reaction, the number of deposition cycles determines the thickness of the film. In the case of TiN, there has been some examination of an initial transient region for TiN, particularly on SiO_2, in which there is a non-linear relationship between number of deposition cycles and film growth [10, 32, 33]. However, little knowledge exists of the chemical reactions that occur on the substrate surface and how this is related to the growth rate of a TiN thin film. Ritala states that steric hindrances alone cannot account for the low growth rate of 1.0 Ti atom/nm^2 that is deposited per cycle [5]. A fraction of a monolayer growth rate is observed for each ALD cycle. This low growth rate was attributed to the

readsorption of the HCl byproduct [5], although other research has shown that HCl is chemisorbed at a surface density of << 1 molecule/10 nm^2 [34]. It has been postulated that during the initial 150 cycles, incoming molecules may react with exposed surface sites on the underlying substrate giving rise to a non-linear growth rate. At the same time, a partially formed layer could hinder the close packing of reactant precursors from the next cycle [10, 15]. Satta also reported that at temperatures at 400ºC and above, 3-D growth of TiN solely on the deposited TiN occurs after only 25 complete cycles [33, 35]. They concluded that a non-linear growth rate during the initial cycles was due to preferential reaction at TiN "islands" [33, 35].

Studies of the formation of TiN on a SiO_2 surface have focused on aspects such as film composition [33], the effects of different SiO_2 substrates [35], and the kinetics of film growth [10, 15]. In order to gain a better grasp of the mechanism of TiN formation on a powder substrate we have used *in situ* FTIR to study the surface species formed during the first six ALD cycles of $TiCl_4$/purge/NH_3/purge on a silica powder. While this approach has been used to elucidate the mechanism of TiO_2 growth on silica powder [30, 31], to the best of our knowledge, a similar study of the substrate-precursor interactions involved in forming TiN on SiO_2 has not been reported.

2. Experimental methods

Fumed silica (Degussa Aerosil A380), with a measured BET surface area of 358 m^2/g, was spread as a thin film on a standard CsI infrared transmission disk. A thin film of silica was used to gain access to the region below 1300 cm^{-1} where characteristic Si-O-Ti, Si-N, Ti-N and Ti-Cl modes lie. The region below 1300 cm^{-1} is opaque when using pressed disks of silica due to absorption by the Si-O bulk modes. The disk was inserted in a heatable, evacuable infrared cell fit with CsI windows [36]. The reference for the thin film of silica was recorded through the thin film just prior to addition of the reagents. All spectra were recorded at 400˚C unless otherwise stated.

IR spectra were recorded on an ABB FTLA 2000 spectrometer equipped with an MCT detector. The disk was placed inside an evacuable IR cell connected to a standard glass vacuum line. All spectra were recorded at 4 cm^{-1} resolution using 100 scans requiring approximately a two-minute collection time. TiN powder, used as obtained from Aldrich, was not amenable to transmission measurement as its large particle size led to scattering of the IR beam. IR spectra of the TiN powder were recorded in DRIFT using a Praying Mantis diffuse reflectance apparatus from Harrick Scientific. KBr powder was used to record the reference for the DRIFT spectra. DRIFT spectra were also recorded at 4 cm^{-1} resolution. Where noted, the spectra were recorded as difference spectra, meaning that positive IR bands arose from addition of bonds to the reference sample and negative bands represent bonds that were removed from the reference sample.

Titanium (IV) tetrachloride from Aldrich (99.9%) and anhydrous ammonia from Matheson Tri-Gas (99.99%) were used as received. The precursors were transferred to evacuable glass flasks. Vapor from the reagents was introduced to the infrared cell using standard vacuum line methods. Precursor vapors were added in an A-B sequence. Approximately 0.4 torr of $TiCl_4$ was added at 400°C for 10 s followed by evacuation of the system to 10^{-5} torr for the A cycle. The B cycle consisted of two NH_3 exposures of approximately 0.5 torr over a three-minute span at 400°C followed by evacuation of the system to a pressure of 10^{-5} torr. Spectra were recorded after each evacuation for every half cycle. Six complete cycles were performed.

3. Results and discussion

3.1 Cycle 1

Figure 1a shows the spectrum of the silica substrate under vacuum at 400ºC (Figure 1a) and the spectra from each half reaction in cycle 1 (Figures 1b and 1c, respectively). The reference for the spectrum of the silica substrate was recorded through the evacuated cell containing the CsI window. This spectrum is the absorbance spectrum of the thin film of silica. In this spectrum, the band at 3742 cm^{-1} is due to the -OH stretching mode of the isolated silanols and the three bands centered at 1096, 809 and 467 cm^{-1} are various Si-O-Si bulk modes.

Figure 1b is the difference spectrum obtained after exposure to $TiCl_4$ vapor for ten seconds at 400ºC followed by evacuation. Note that the reference for this spectrum was recorded through the silica film just prior to addition of the gaseous $TiCl_4$. The intensity of the negative band at 3742 cm^{-1} is equivalent in intensity to the positive peak at 3742 cm^{-1} in Figure 1a, and, thus, the reaction of $TiCl_4$ was rapid and complete as was demonstrated by Lakomaa [17] and others [30, 31]. The positive bands at 992 and 909 cm^{-1} are assigned to the Si-O-Ti stretching modes of monodentate and bidentate $(Si\text{-}O)_n\text{-}TiCl_{4-n}$ groups, (where n = 1, 2 for monodentate and bidentate peaks, respectively) [17, 19, 20, 30, 31]. Bands at 767 and 715 cm^{-1} are due to formation of multiply bonded Ti-O species [37]. These bands could also be due to partial hydrolysis of the surface $TiCl_x$ species with rogue water in the vacuum line. A band at 500 cm^{-1} indicates the presence of Ti-Cl_x surface species. The IR spectra obtained in the first half-cycle is in agreement with the results of others [5, 30, 31, 38] showing that the overall reaction is:

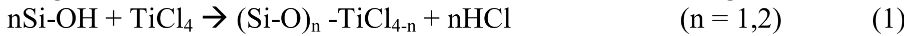

$$nSi\text{-}OH + TiCl_4 \rightarrow (Si\text{-}O)_n\text{-}TiCl_{4-n} + nHCl \qquad (n = 1,2) \qquad (1)$$

It has been shown that the relative amount of monodentate and bidentate species is reaction temperature-dependent. Blitz *et al.* showed that monodentate species are favored at higher reaction temperature [39] while Lakomaa *et al.* and Greer *et al.* state that bidentate species are favored at this reaction temperature [17, 32]. In our case, bands at 992 and 909 cm^{-1} show that both types of Si-O-Ti bonds appear after the first half cycle.

In the second half cycle, ammonia was added for approximately three minutes at 400ºC, and the sample cell was then evacuated. The difference spectrum recorded is shown in Figure 1c. Positive bands appearing at 3440 and 1556 $cm^{-1}$are due to N-H stretching and bending modes, respectively. The frequency position of these bands are consistent with the formation of a surface M_2–NH group with either two silicon atoms [40, 41], two titanium atoms or one of each. The reaction with ammonia at the surface is accompanied by the removal of the Ti-Cl_x band at 500 cm^{-1} which shows that the reaction of ammonia occurs with the Ti-Cl_x groups and thus the most likely M_2-NH species is Ti_2-NH. A reaction between Ti-Cl_x surface groups and ammonia is supported by the appearance of -NH peaks at 3440 and 1556 cm^{-1}. A primary amine which has bands between 3450-3490 and between 3530 and 3580 cm^{-1} as stated by Peri [34]. Furthermore, the reaction of ammonia with silica at temperatures greater than 300ºC leads to the appearance of a secondary –NH peak at 3440 cm^{-1} [41] The NH_4Cl is a byproduct of the reaction between NH_3 and HCl generated in the reaction as seen through the appearance of peaks at 3137, 3047, 2805, and 1404 cm^{-1} and corresponds well with Kiselev [41] and Hamann [42]. The salt sublimes from the silica surface between 400 and 600ºC and forms -NH_2 groups on the surface [14, 34].. Elers states that NH_4Cl will decompose at temperatures greater than 370ºC and may leave chlorine residue on the surface [43]. The absence of -NH_2 surface groups in the silica spectra leads to the belief that the observed NH_4Cl salt must have formed on the IR windows. Tripp and Hair report that surface salt is removed from the spectrum under vacuum at 200ºC [44].

We now return to the question of whether TiN is formed. Figure 1c also shows a strong, broad mode at 670 cm^{-1}, and this band position is consistent with formation of Ti-N. However, this

assignment could be debated as TiO_2 also produces a broad band in the same region. To resolve this question we refer to the data presented in Figure 2. Figure 2a is a replot of Figure 1c and is provided for comparative purposes. Figure 2b is the spectrum obtained in a separate experiment in which water vapor was added instead of ammonia in step B of cycle 1. The substitution of water vapor for ammonia leads to the growth of a TiO_2 layer on the surface [17, 19, 30]. In this case, there are clear differences between Figures 2a and b in the region where TiN and TiO_2 bands are expected. The growth of TiO_2 leads to a broad band centered at a slightly higher position (700 cm^{-1}) than the 670 cm^{-1} peak in Figure 2a and is accompanied by a second band near 373 cm^{-1}. This second band is not observed in Figure 2a. For comparison, Figures 2c and 2d are IR spectra of TiN and TiO_2 powder, respectively. TiO_2 powder, again, has a broad band near 700 cm^{-1} and a second band at 317 cm^{-1} whereas TiN has a single broad peak centered at 670 cm^{-1}. Also note a similar shape to the TiN band at 670 cm^{-1} in both Figures 2a and 2c. For example, both spectra have shoulder bands located at 759 and 511 cm^{-1}. Therefore, the spectra in Figure 2 support an assignment of the 670 cm^{-1} peak to growth of TiN on the surface.

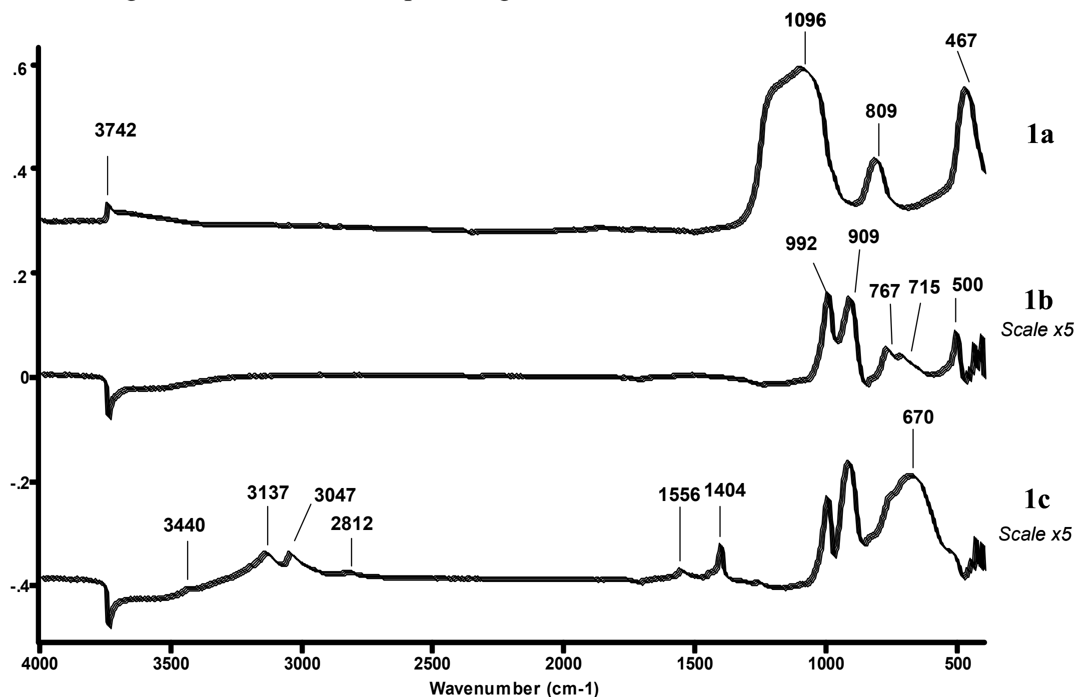

Figure 1. Thin film IR spectra of silica substrate (a) and Cycle 1 first exposure of $TiCl_4$ (b), and first exposure of NH_3 (c)

However, the reaction of ammonia in cycle 1 is more complicated than just reaction with the Ti-Cl_x groups leading to formation of Ti_2NH and TiN. It is noted that the addition of ammonia also leads to a decrease in the Si-O-Ti bands at 992 and 902 cm^{-1} which shows that there is some cleavage of the Si-O-Ti bond. This is more clearly seen in Figure 3a which is the difference spectrum of the B step in cycle 1 using the A step of cycle 1 as a reference. The removal of Si-O-Ti bonds is accompanied by the re-emergence of the Si-OH band at 3742 cm^{-1}. The intensity of this band is about 28% of the original silanols' intensity. Thus, we conclude that a secondary reaction occurs with ammonia in which a portion of the surface $(SiO)_nTiCl_{4-n}$ (n=1,2) are cleaved and the Si-O group is hydrogenated by ammonia reforming isolated Si-OH groups. This behavior with ammonia is similar to the addition of water vapor which also led to a partial cleavage of the

Si-O-Ti bond and reformation of Si-OH groups [30]. The work of Chapman and Hair showed that treating silica with ethanolamine removed the isolated Si-OH peak. Subsequent evacuation of the surface removed adsorbed molecules and lead to the partial restoration of the peak at temperatures from 100 to 200ºC [40]. It is also found that the number of Si-OH groups returning decreases with each cycle. While 28% of the Si-OH groups reform at the end of cycle 1, 15% of the Si-OH groups regenerate after the second cycle. From the third to sixth cycles, no Si-OH regeneration was observed.

To recap, in the first half cycle, the isolated silanol groups have been removed from the surface, while covalent monodentate and bidentate $(Si\text{-}O)_nTi\text{-}Cl_{4-n}$ (n=1,2) species are formed. In the second half cycle, the main reaction occurs between ammonia and the $Ti\text{-}Cl_x$ groups leading to TiN terminated with Ti_2-NH surface groups. There is a secondary reaction with the ammonia resulting in some cleavage of the $(Si\text{-}O)_nTiCl_{4-n}$ groups at the Si-O-Ti bond and reformation of isolated Si-OH groups.

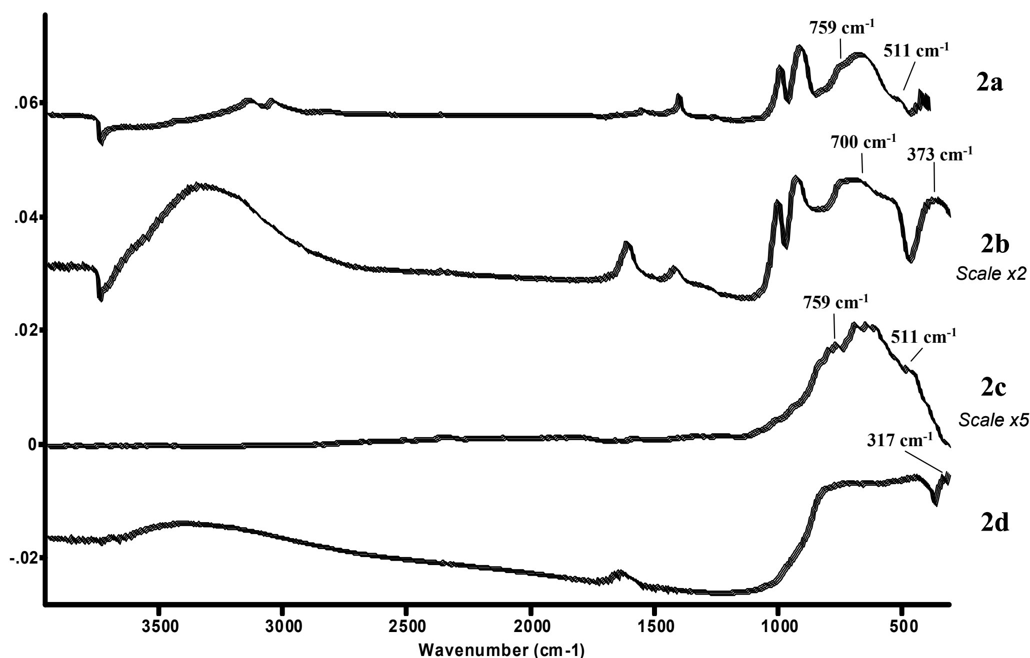

Figure 2. IR spectra of the first exposure of NH_3 (a) compared with TiO_2 ALD on silica (b), DRIFT IR spectra on TiN standard powder (c), and Degussa P25 TiO_2 (d)

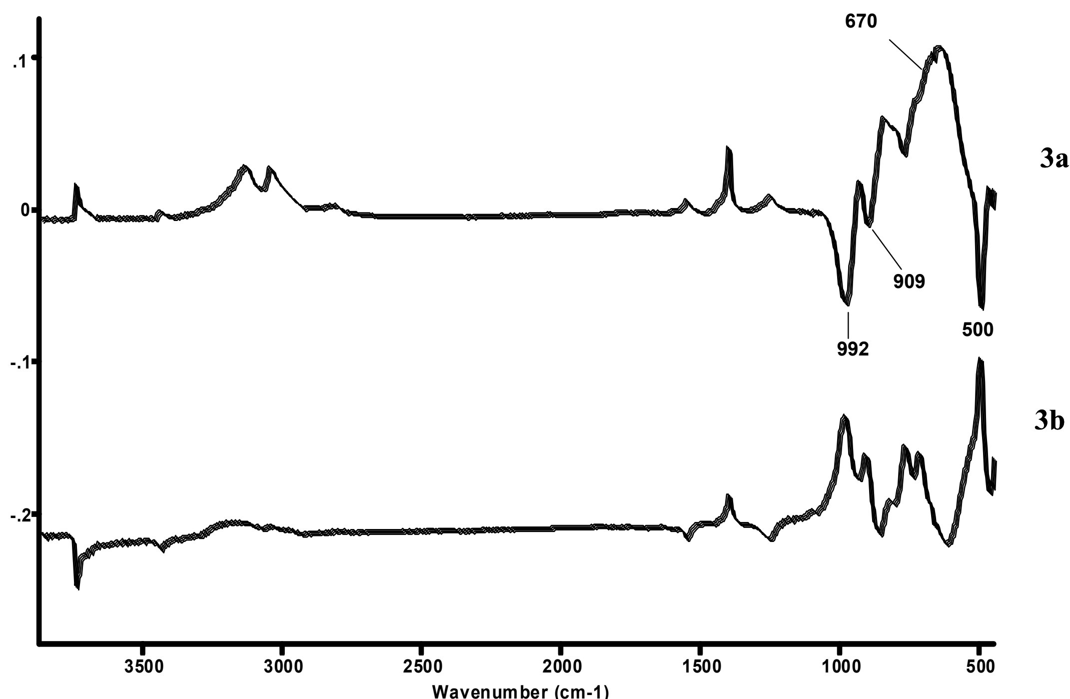

Figure 3. Difference IR spectrum of the first NH_3 exposure using a reference spectrum of the first exposure of $TiCl_4$ (1c – 1b) (a), and the difference spectrum of the second $TiCl_4$ exposure using a reference of the first exposure to NH_3 (b)

3.2 Cycle 2 and higher

Figure 3b is the difference spectrum recorded for $TiCl_4$ addition in cycle 2. In this case the reference is the single beam spectrum after ammonia addition in the first cycle. In other words, this spectrum shows the difference in reaction of the $TiCl_4$ with the underlying layer produced at the end of cycle 1. The spectrum contains bands due to reaction with the TiN layer as well as bands due to reaction with exposed sites on the underlying silica. Reaction with the underlying silica is evidenced by the negative band at 3742 cm^{-1} along with positive Si-O-Ti bands at 992 and 909 cm^{-1} and Ti-Cl_x at 500 cm^{-1}. This shows that the Si-OH groups that reformed with the addition of ammonia in cycle 1 again reacted with the $TiCl_4$ giving rise to $(Si\text{-}O)_nTiCl_{4-n}$ (where n=1,2) groups. As mentioned earlier, this above reaction only occurs during the first three cycles where there is a transition from the silica to a TiN surface. With each cycle, the number of Si-OH groups reforming with addition of ammonia diminishes and does not appear after the third complete cycle.

There are several peaks in Figure 3b that indicate reaction of $TiCl_4$ with the underlying TiN surface. These changes appear in cycle 2 and occur each time in higher cycles. The negative bands at 3440 cm^{-1} and 1556 cm^{-1} show that the surface Ti_2–NH groups react with incoming $TiCl_4$ molecules. While the Ti-Cl_x band at 500 cm^{-1} in Figure 3a is partially due to $(SiO)_nTiCl_{4-n,}$, the reaction of $TiCl_4$ with the Ti_2NH also produces a Ti-Cl_x band at 500 cm^{-1} Comparison of the integrated peak areas (not shown) of the Ti-Cl_x and –NH bands shows a consistent increase and decrease with each cycle. However, during a typical half-cycle, only 30-40% of the surface

species is removed. There is no increase in the TiN peak at 670 cm^{-1} and bands due to multiply bonded Ti-O bands, [37] at 767 and 715 cm^{-1}, again appear. In addition, NH_4Cl is formed as a byproduct as the bands at 3137, 3047, 2812, and 1404 cm^{-1} increase in intensity.

Figures 4 and 5 are IR spectra recorded after the first, second and sixth ALD cycles for the A step and B step, respectively. As mentioned above, after the initial transition phase, the reaction of $TiCl_4$ in step A of each cycle involves a reaction with the Ti_2-NH groups producing an adsorbed $TiCl_x$ species. During step A, there is no change in intensity of the TiN band at 670 cm^{-1} or the intensity of the bands due to NH_4Cl. The most significant change occurs between cycle 1 (Figure 4a) and cycle 2 (Figure 4b). The spectrum for the sixth cycle varies little in appearance as all surface groups are present.In step B, the addition of ammonia leads to a decrease in the Ti-Cl band at 500 cm^{-1} and this is accompanied by the reappearance of bands at 3440 and 1556 cm^{-1} due to Ti_2NH and an increase in intensity of the TiN band at 670 cm^{-1}. NH_4Cl is also formed during step B of each cycle. Minimal change to the spectra is seen.

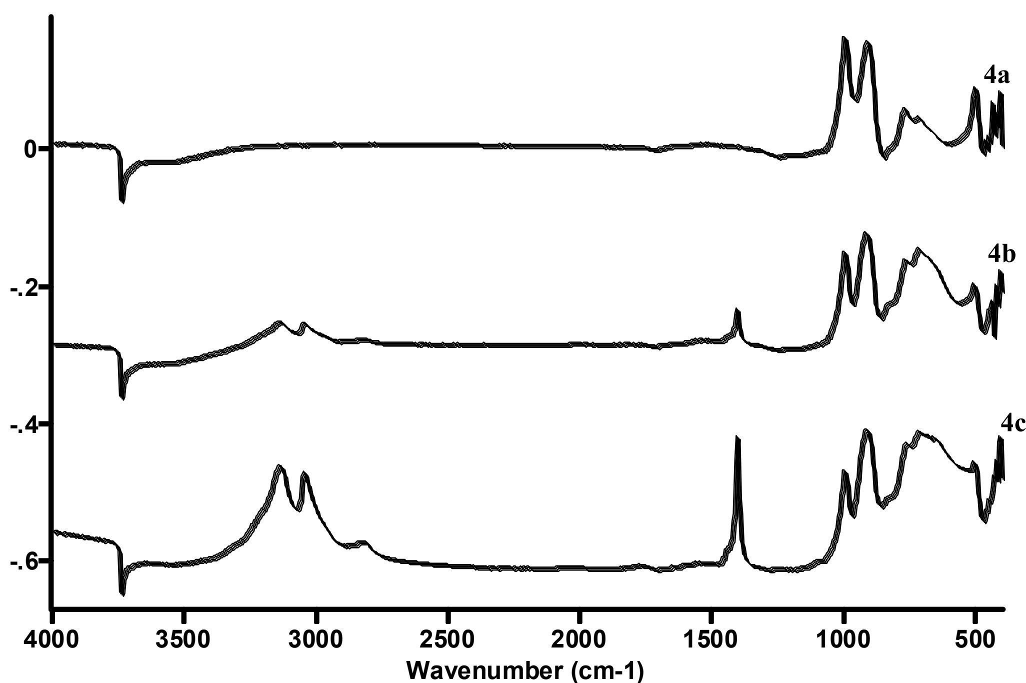

Figure 4. IR spectra of cycles 1 (a), 2 (b), and 6 (c) for step A ($TiCl_4$ addition) for each cycle using the silica substrate as a reference

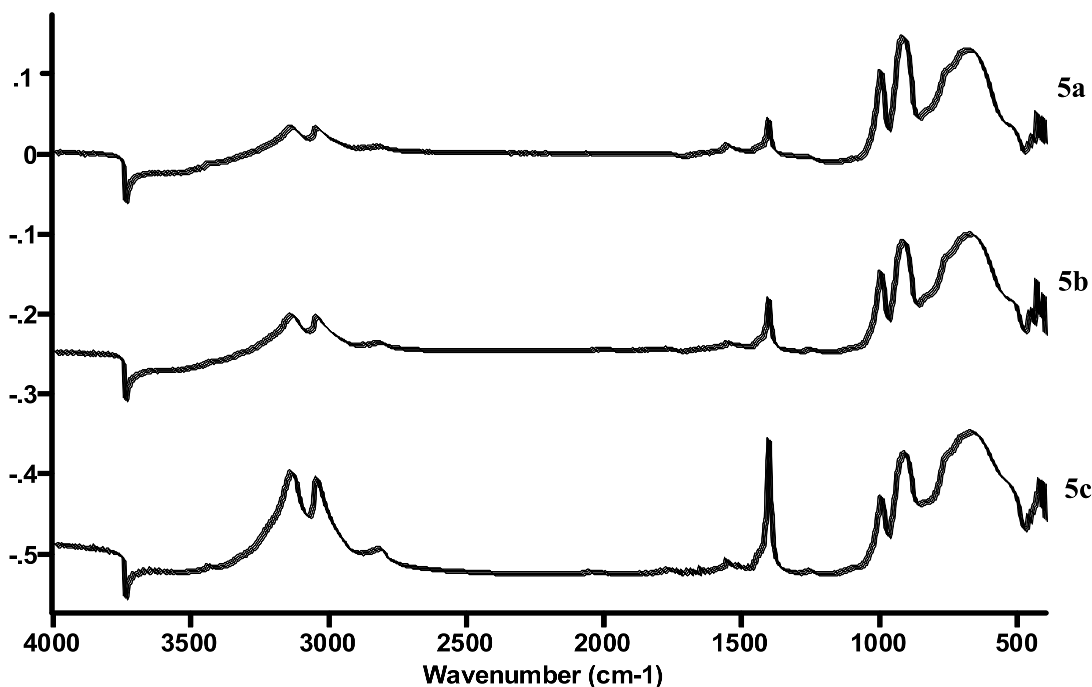

Figure 5. IR spectra of cycles 1 (a), 2 (b), and 6 (c) for step B (NH_3 addition) for each cycle using the silica substrate as a reference

Figure 6 is a plot of the change in integrated peak area for bands representing mono- and bidentate Si-O-Ti, Si-OH, and TiN as a function of the number of ALD cycles. During the first two cycles we observe a non-linear growth in TiN along with changes in the Si-O-Ti bands. The decrease in intensity of the Si-O-Ti band shows that reformation of Si-OH groups occurs through cleavage by gaseous NH_3 of the monodentate $SiOTiCl_3$ and bidentate $(SiO)_2TiCl_2$ species. This was also found with addition of H_2O vapor instead of NH_3 [30]. After the transition cycles (2-3 cycles), growth of TiN bands is linear with each ALD cycle and there is little reaction with the underlying silica as evidenced by the almost constant intensity of the Si-O-Ti bands. The rapid rate of formation of Si-O-Ti bonds [30] and the low growth rate of TiN by ALD has been noted in the literature [5]. Three-dimensional growth has been observed at this temperature, thus leading to a relatively constant amount of the surface species even though TiN is accumulating [33]. Furthermore, adsorbed molecules prevent subsequent reactant molecules from close-packing resulting in the formation of intervals larger than required for a TiN molecule in the transient region of the film [15]. Additionally, the spectral evidence of incomplete removal of Cl and H ligands, which supports the suggestion of Ritala [5], as well as reformation of surface silanols, demonstrates that the low growth rate may be related to incomplete surface reactions.

The above results lead to a proposed mechanism consistent with the data for the creation of a TiN thin film. In this reaction, the $TiCl_4$ vapor reacts with the surface silanol groups and form $TiCl_2$ and $TiCl_3$ molecules [17] that are covalently bonded to the surface via Si-O-Ti bonds. HCl gas is formed as a by-product and purged from the reactor. Addition of NH_3 creates a bond with covalent and metallic properties [45] resulting in a Ti_2NH compound. Once the silica surface has been saturated with the Ti_2NH compound, it reoccurs on top of the preceding layer. All successive reactions can be illustrated by Figure 7.

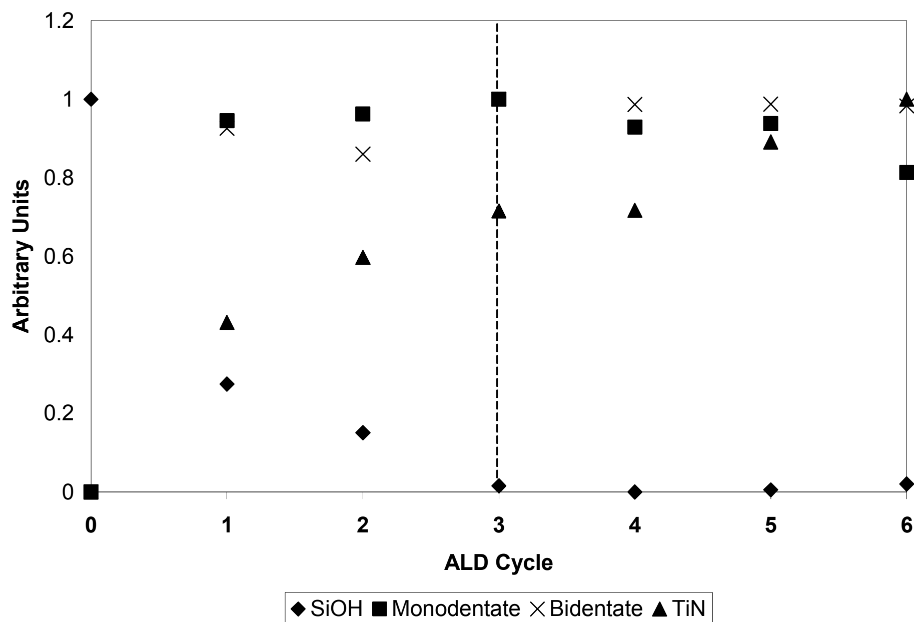

Figure 6. Comparison of normalized peak area vs. number of ALD cycles for various bands

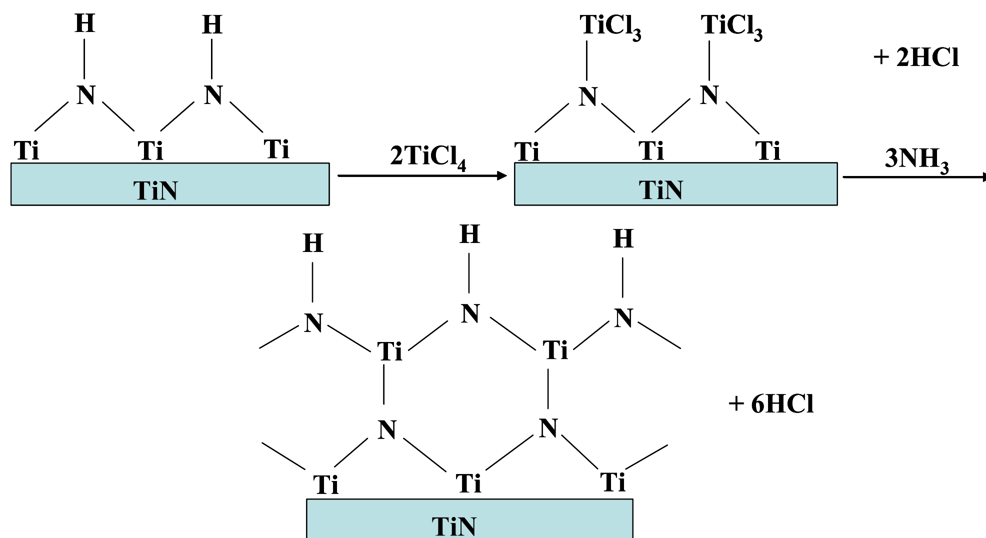

Figure 7. Reaction scheme for TiN formation

4. Conclusions

The initial stages of titanium nitride atomic layer deposition on silica powder were investigated using *in situ* FTIR techniques. There is a transition between a silica and TiN-covered surface that requires about three ALD cycles. During the first complete cycle, Si-O-Ti bond formation is

observed indicating that titanium atoms have been covalently attached to the silica surface through $(SiO)_n$-$TiCl_{4-n}$ (where n=1,2). Reaction with NH_3 in step B leads to a reaction with the above species leading to Ti_2NH and TiN. A secondary reaction occurs where the NH_3 cleaves the adsorbed species via the Si-O-Ti bond resulting in the reformation of Si-OH groups. After the first two to three cycles, the reaction proceeds through reaction of gaseous $TiCl_4$ with Ti_2NH to yield adsorbed Ti-Cl_x species, and the reaction of NH_3 in step B with this species to form TiN and Ti_2NH. Reappearance of Si-OH groups with the addition of NH_3 and incomplete surface reactions between Ti-Cl_x groups and –NH groups help to explain the low TiN growth rate.

References

[1] Y. Mochizuki, Y. Okamoto, A. Ishitani, K. Hirose, and T. Takada, Japanese Journal of Applied Physics, Part 2: Letters 34 (1995) L326.
[2] H. De Baynast, A. Bouteville, and J.-C. Remy, Chemical Vapor Deposition 6 (2000) 115.
[3] J. N. Musher and R. G. Gordon, Journal of the Electrochemical Society 143 (1996) 736.
[4] T. Tanaka, T. Nakajima, and K. Yamashita, Thin Solid Films 409 (2002) 51.
[5] M. Ritala, M. Leskelae, E. Rauhala, and P. Haussalo, Journal of the Electrochemical Society 142 (1995) 2731.
[6] C. H. Winter, J. W. Proscia, A. L. Rheingold, and T. S. Lewkebandara, Inorganic Chemistry 33 (1994) 1227.
[7] M. Grujicic and S. G. Lai, Journal of Materials Science 36 (2001) 2937.
[8] S. Ishihara and M. Hanabusa, Journal of Applied Physics 84 (1998) 596.
[9] A. Berry, R. Mowery, N. H. Turner, L. Seitzman, D. Dunn, and H. Ladouceur, Thin Solid Films 323 (1998) 10.
[10] J.-W. Lim, J.-S. Park, and S.-W. Kang, Journal of Applied Physics 87 (2000) 4632.
[11] M. Ritala, T. Asikainen, M. Leskela, J. Jokinen, R. Lappalainen, M. Utriainen, L. Niinisto, and E. Ristolainen, Applied Surface Science 120 (1997) 199.
[12] Y. J. Lee and S.-W. Kang, Journal of Vacuum Science & Technology, A: Vacuum, Surfaces, and Films 21 (2003) L13.
[13] J. Kim, H. Hong, K. Oh, and C. Lee, Applied Surface Science 210 (2003) 231.
[14] J. W. Elam, M. Schuisky, J. D. Ferguson, and S. M. George, Thin Solid Films 436 (2003) 145.
[15] J.-W. Lim, H.-S. Park, and S.-W. Kang, Journal of the Electrochemical Society 148 (2001) C403.
[16] J.-S. Min, Y.-W. Son, W.-G. Kang, S.-S. Chun, and S.-W. Kang, Japanese Journal of Applied Physics, Part 1: Regular Papers, Short Notes & Review Papers 37 (1998) 4999.
[17] E. L. Lakomaa, S. Haukka, and T. Suntola, Applied Surface Science 60-61 (1992) 742.
[18] S. Haukka, E. L. Lakomaa, O. Jylha, J. Vilhunen, and S. Hornytzkyj, Langmuir 9 (1993) 3497.
[19] S. Haukka, E. L. Lakomaa, and T. Suntola, Thin Solid Films 225 (1993) 280.
[20] S. Haukka, E. L. Lakomaa, and A. Root, Journal of Physical Chemistry 97 (1993) 5085.
[21] M. Lindblad, S. Haukka, A. Kytoekivi, E.-L. Lakomaa, A. Rautiainen, and T. Suntola, Applied Surface Science 121/122 (1997) 286.
[22] S. Haukka, E. L. Lakomaa, and T. Suntola, Studies in Surface Science and Catalysis 120A (1999) 715.
[23] S. I. Kol'tsov and V. B. Aleskovskii, Zhurnal Prikladnoi Fiziki 40 (1967) 907.
[24] A. M. Shevyakov, G. N. Kuznetsova, and V. B. Aleskovskii, Khim. Vysokotemp. Mater., Tr. Vses. Soveshch., 2nd 149-55 (1965) 149.
[25] L. A. Sergeeva, I. P. Kalinkin, and V. B. Aleskovskii, Izvestiya Leningradskogo Elektrotekhnicheskogo Instituta imeni V. I. Ul'yanova No. 57 (1966) 103.
[26] R. L. Puurunen, Journal of Applied Physics 97 (2005) 121301/1.
[27] J. D. Ferguson, A. W. Weimer, and S. M. George, Chemistry of Materials 12 (2000) 3472.
[28] J. R. Wank, S. M. George, and A. W. Weimer, Powder Technology 121 (2001) 195.
[29] J. R. Wank, S. M. George, and A. W. Weimer, Journal of the American Ceramic Society 87 (2004) 762.
[30] W. Gu and C. P. Tripp, Langmuir 21 (2005) 211.

[31] B. J. Ninness, D. W. Bousfield, and C. P. Tripp, Colloids and Surfaces, A: Physicochemical and Engineering Aspects 214 (2003) 195.
[32] F. Greer, D. Fraser, J. W. Coburn, and D. B. Graves, Journal of Vacuum Science & Technology, A: Vacuum, Surfaces, and Films 21 (2003) 96.
[33] A. Satta, J. Schuhmacher, C. M. Whelan, W. Vandervorst, S. H. Brongersma, G. P. Beyer, K. Maex, A. Vantomme, M. M. Viitanen, H. H. Brongersma, and W. F. A. Besling, Journal of Applied Physics 92 (2002) 7641.
[34] J. B. Peri, Journal of Physical Chemistry 70 (1966) 2937.
[35] A. Satta, A. Vantomme, J. Schuhmacher, C. M. Whelan, V. Sutcliffe, and K. Maex, Applied Physics Letters 84 (2004) 4571.
[36] C. P. Tripp and M. L. Hair, Langmuir 7 (1991) 923.
[37] D. T. Molapo, University of Ottawa, Ottawa, 1998.
[38] M. Juppo, P. Alen, M. Ritala, T. Sajavaara, J. Keinonen, and M. Leskela, Electrochemical and Solid-State Letters 5 (2002) C4.
[39] J. P. Blitz, Colloids and Surfaces 63 (1992) 11.
[40] I. D. Chapman and M. L. Hair, Transactions of the Faraday Society 61 (1965) 1507.
[41] A. V. Kiselev, Lygin, V. I., Infrared Spectra of Surface Compounds, John Wiley & Sons, Inc., Jerusalem, 1975.
[42] S. D. Hamann, Australian Journal of Chemistry 31 (1978) 919.
[43] K.-E. Elers, V. Saanila, P. J. Soininen, W.-M. Li, J. T. Kostamo, S. Haukka, J. Juhanoja, and W. F. A. Besling, Chemical Vapor Deposition 8 (2002) 149.
[44] C. P. Tripp and M. L. Hair, Journal of Physical Chemistry 97 (1993) 5693.
[45] H. G. Tompkins, Journal of Applied Physics 70 (1991) 3876.

Synthesis and Characterization of TiN Thin Coatings on SiO_2 and $Li_4Ti_5O_{12}$ Nanoparticles

1. Introduction

Titanium nitride (TiN) is a conducting, refractory material that has found a variety of applications as a thin film. TiN thin films have been widely used as diffusion barriers for metal interconnects in ULSI processing [1-3], cutting tools, solar films for windows and even for decorative purposes[4, 5]. Another potential application is in the area of surface passivation of electrode material in high-energy density lithium-ion batteries. The use of smaller electrode particles to create a higher energy density in lithium-ion batteries is challenging because of the high electrochemical reactivity of these surfaces towards electrolytes, particularly at higher voltages. The high conductivity of TiN along with its potential to diffuse lithium ions makes it an attractive candidate for passivating the surface of smaller electrode particles and thus opening up the use of higher surface electrode material in high energy lithium-ion batteries.

Titanium nitride thin films have been deposited by a variety of techniques including physical vapor deposition (PVD) [2], chemical vapor deposition (CVD) [1-3, 6], and atomic layer deposition (ALD) [4, 7, 8], techniques. Of these techniques, CVD and ALD are preferred for coating non-planar surfaces like those of trenches and particles. ALD consists of two consecutive half-reactions that each proceed until surface saturation occurs. The second half-reaction completes one saturated surface layer of the thin film being deposited. Repetition of these reaction cycles lead to the build-up of a continuous thin film[4, 9, 10]. Because of the monolayer control of film growth, ALD is well-suited for uniform deposition on non-planar supports, including nanoparticle coating. An additional benefit of ALD is that reaction temperatures are typically lower than CVD [4, 10]. This lower reaction temperature will minimize particulate sintering and surface area reduction in nanoparticles.

The ALD of TiN typically involves the two-step reaction of $TiCl_4$ and NH_3 at 400°C [10-12]. In addition, Gordon first published on the use of dimethylamido metal compounds as low temperature precursors for TiN chemical vapor deposition [13]. These dimethylamido compounds work well for forming other metal nitrides as well [14, 15], although the reactions are not as chemically clean as the $TiCl_4$ and NH_3 process. Similar research into ALD of AlN has been carried out including an interesting report of coating silica particles for catalyst support applications [16]

ALD has been recently used to coat the surfaces of powders with SiO_2 [17] and Al_2O_3 [18]. It was shown that uniform, conformal coatings could be achieved using ALD. In this work, we report the preparation and characterization of TiN thin films on nanoparticles of Si and $Li_4Ti_5O_{12}$, both anode materials used in lithium-ion batteries. The coatings were prepared by ALD using $TiCl_4$ and NH_3 as reactants. The ALD process and coatings were characterized by Fourier transform infrared spectroscopy (FTIR), nitrogen analysis, x-ray photoelectron spectroscopy (XPS) and transmission electron microscopy (TEM).

2. Experimental

ALD Reactor System The atomic layer deposition reactor consists of one stainless steel bubbler to supply the $TiCl_4$ (Aldrich, 99.9%) precursor, while anhydrous ammonia (Matheson Tri-Gas, 99.99%) is supplied by a tank, pressurized to 40 psi. Air-actuated valves regulate precursor delivery. $TiCl_4$ flow was controlled by holding its temperature to 0ºC giving it a vapor pressure of approximately 2.5 Torr. Ammonia flow was controlled by a MKS mass flow controller with a

flow rate of 20 sccm. The deposition cell is a vertically mounted quartz tube with a porous frit centered axially within the tube to act as a support platform for the powder substrate while allowing the excess precursors to exit the deposition area. A muffle furnace held the reaction temperature at 425ºC. The run and vent lines to and from the reactor were electrically heated at 250ºC to prevent condensation and formation of a $TiCl_4$:NH_3 adduct. The pressures upstream and downstream of the reactor were monitored with Baratron differential pressure gauges. The system was equipped with a mechanical vacuum pump and liquid nitrogen trap. All pneumatic valves are actuated via computer software.

ALD Reaction The ALD reaction was performed using either 0.30 g of lithium titanate spinel (Altair) powder, 0.08 g of silicon powder from Lithion, Inc.(84% Si, 2% SAB C, 2% Sup P, 2% KS15 by weight) or 0.05 g of silica nanospheres as substrates. The substrate was exposed to 5 x 10^6 Langmuirs (L) of $TiCl_4$ followed by a three-second evacuation and a two-second nitrogen purge for the first half-cycle. Subsequently, the supports were exposed to 1.2 x 10^9 L NH_3 followed by a three-second evacuation and a two-second purge. This reaction sequence was repeated up to 1000 times to achieve an appreciable thin film and run at temperatures of 500ºC, 550ºC, and 600ºC. Immediately after the TiN-coated sample was removed from the reaction chamber it was placed in a pyrex tube and sealed under vacuum to minimize the sample's exposure to oxygen.

Material Characterization

In-situ FTIR Fumed silica (Degussa Aerosil A380), with a measured BET surface area of 358 m^2/g, was spread as a thin film on a standard CsI infrared transmission disk. A thin film of silica was used to gain access to the region below 1300 cm^{-1} where characteristic Si-O-Ti, Si-N, Ti-N and Ti-Cl modes lie. The region below 1300 cm^{-1} is opaque when using pressed disks of silica due to absorption by the Si-O bulk modes. The disk was inserted in a heatable, evacuable infrared cell fit with CsI windows [19]. The reference for the thin film of silica was recorded through the thin film just prior to addition of the reagents. All spectra were recorded at 400˚C unless otherwise stated.

IR spectra were recorded on an ABB FTLA 2000 spectrometer equipped with an MCT detector. The disk was placed inside an evacuable IR cell connected to a standard glass vacuum line. All spectra were recorded at 4 cm^{-1} resolution using 100 scans requiring approximately a two-minute collection time. TiN powder, used as obtained from Aldrich, was not amenable to transmission measurement as its large particle size led to scattering of the IR beam. IR spectra of the TiN powder were recorded in DRIFT using a Praying Mantis diffuse reflectance apparatus from Harrick Scientific. KBr powder was used to record the reference for the DRIFT spectra. DRIFT spectra were also recorded at 4 cm^{-1} resolution. Where noted, the spectra were recorded as difference spectra, meaning that positive IR bands arose from addition of bonds to the reference sample and negative bands represent bonds that were removed from the reference sample.

Titanium (IV) tetrachloride and anhydrous ammonia were used as received. The precursors were transferred to evacuable glass flasks. Vapor from the reagents was introduced to the infrared cell using standard vacuum line methods. Precursor vapors were added in an A-B sequence. Approximately 0.4 torr of $TiCl_4$ was added at 400°C for 10 s followed by evacuation of the system to 10^{-5} torr for the A cycle. The B cycle consisted of two NH_3 exposures of approximately 0.5 torr over a three-minute span at 400°C followed by evacuation of the system to a pressure of 10^{-5} torr. Spectra were recorded after each evacuation for every half cycle. Six complete cycles were performed.

Nitrogen analysis Modified powder samples were completely combusted at 1350ºC. The conductivity of the resulting NO_x combustion products was measured to determine the total nitrogen content.

TEM A Philips CM-10 tunneling electron microscope with 100-kV beam at 3.4 x 10^5 times magnification was used to examine powder samples. All samples were mounted on a copper grid with a carbon backing.

3. Results

In situ IR spectroscopy was used to study the first six ALD cycles to verify the presence of TiN on the substrate surface and gain an understanding of the film growth mechanism. Figure 1a shows the difference spectrum taken after one complete ALD cycle ($TiCl_4$ exposure, purge, NH_3 exposure, purge) with a background of silica powder at 400ºC. The negative peak at 3742 cm^{-1} represents the removal of isolated Si-OH groups from the surface through the addition of $TiCl_4$. The small positive bands at 3440 and 1556 cm^{-1} indicate the formation of secondary –NH groups on the surface. Formation of Si-O-Ti groups on the SiO_2 surface is seen by the peaks at 992 cm^{-1} (bidentate bonds, $(SiO\text{-})_2\text{-O-TiCl}_2$) and 909 cm^{-1} (monodentate bonds, SiO-$TiCl_3$). A broad peak then appears centered around 670 cm^{-1} with shoulders at 759 cm^{-1} and 511 cm^{-1}. This is believed to be TiN. The peaks at 3137, 3047, 2812, and 1404 cm^{-1} are attributed to the formation of NH_4Cl on the CsI window. Salt formation is a byproduct of the reaction between $TiCl_4$ and NH_3 [20] and is sublimed between 400ºC and 600 ºC [21]. DRIFT IR was performed on TiN powder for the

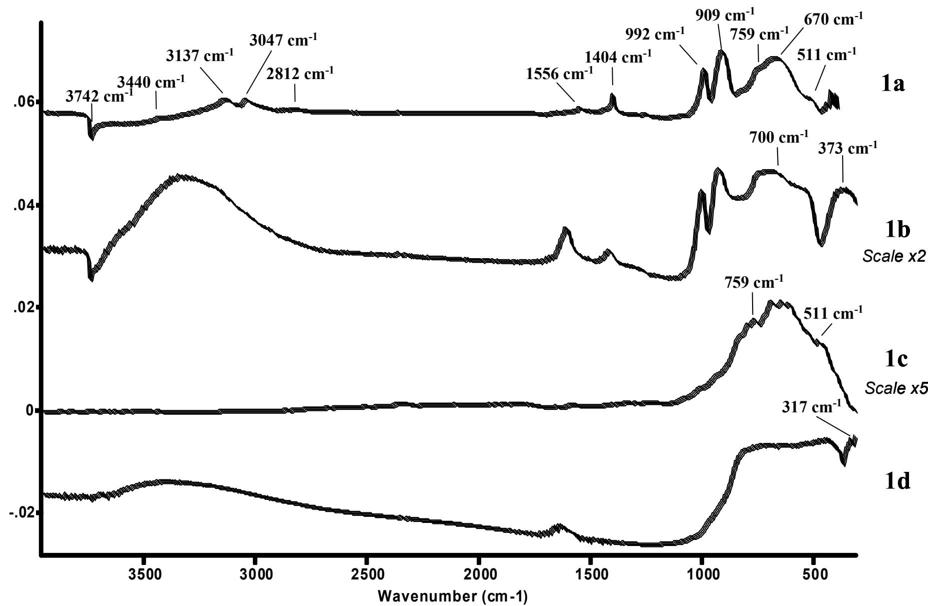

Figure 1: FTIR spectra of (a) TiN ALD *in situ* on SiO2 powder (SiO2 background at 400ºC) (b) TiO2 ALD *in situ* on SiO2 powder (c) DRIFT IR spectrum of TiN powder in KBr and (d) FTIR spectrum of P25 TiO2 powder.

sake of comparison and can be seen in Figure 1c. A similar pattern is seen in the location of the peak and the presence of the two shoulders (759 and 511 cm^{-1}). The presence of water in the vacuum manifold could lead to the formation of TiO_2 which also is found in this region of the spectrum. Figure 1b is the spectrum of TiO_2 formed through ALD on the same silica substrate during a different experiment. Instead of using ammonia in the B step, H_2O was used [22]. Examination of Figure 1b shows that the broad band for TiO_2 is centered around 700 cm^{-1} with another band at 373 cm^{-1}. This second band is not seen if Figure 1a. The spectrum of P25 TiO_2

powder (DeGussa) is displayed in Figure 1d. Again, a broad band centered around 700 cm^{-1} is the dominant feature with a second band at 317 cm^{-1}. The comparison of the spectrum in Figure 1a with that of Figure 1c and subsequent contrasts with the spectra in Figures 1b and 1d support the assignment of the peak at 670 cm^{-1} to TiN growth and its covalent bonding with the SiO_2 substrate. Due to the conductivity of the lithium titanate spinel, this *in situ* analysis could not be performed.

In addition to $Li_4Ti_5O_{12}$ and Si powder, SiO_2 nanospheres were coated with TiN by ALD to examine the ability of ALD to conformally coat a well-defined nanosphere. A TEM is included (Figure 2) of unmodified and modified SiO_2 nanospheres to show the change in appearance of the surface. The unmodified spheres (Figure 2a) appear to have a smooth surface. The image of the sphere becomes increasingly darker moving from the perimeter of the sphere to its core. Examination of the modified spheres (Figure 2b) indicates the presence of granular structures on the surface. A dark, dense halo appears around the perimeter of the sphere, along with the appearance of crystallites on the surface. The observed change is consistent with the formation of a thin layer on the surface of the particle. The thickness of the film, estimated at 27 Å, or 0.14 Å/cycle, is slightly less than thicknesses observed for thin films deposited on planar silica substrates at similar reaction conditions [4].

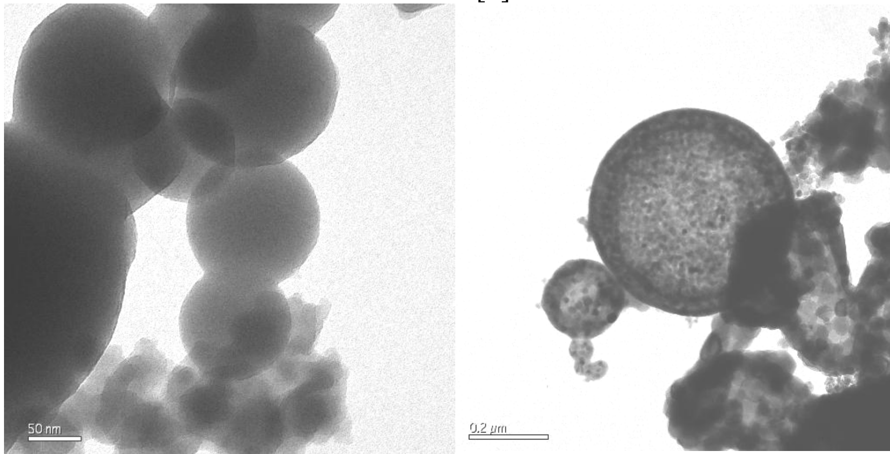

Figure 2: (a) uncoated silica nanospheres and (b) TiN-coated silica nanospheres.

In the data analysis, it is important to note that the surface of TiN will oxidize as the free energy of oxidation at room temperature is -128 kcal/mol, and, therefore, spontaneous. XPS on TiN standard material (Aldrich) that was stored in ambient conditions indicated that there was significant oxidation of the surface. In our experiments we consistently stored our samples under vacuum immediately after preparation, in attempts to both minimize oxidation and minimize the randomness in the amount of oxidation from sample to sample. We used nitrogen analysis to determine the relative amount of TiN on the surface of the nanoparticle. This may have slightly underestimated the total TiN quantity due to small amounts of oxidation. [23].

Five hundred layers of TiN were deposited on Si and $Li_4Ti_5O_{12}$ at temperatures of 500ºC, 550ºC, and 600ºC. The Si powder appeared to change to a bronze color from its original gray-brown color due to the deposition of TiN. The reaction temperature affected the color of the $Li_4Ti_5O_{12}$ powder. After depositing 500 layers at 500ºC, the $Li_4Ti_5O_{12}$ powder was tan, appearing darker at the top of the sample, closer to the inlet, than at the bottom. At 550ºC, the product was brown at the top and green-gray at the bottom. The $Li_4Ti_5O_{12}$ powder reacted at 600ºC was a reddish brown color.

Figure 3 shows the relationship between film quantity estimated by nitrogen analysis and temperature. The growth rate of TiN was thermally activated on both powders. The lower growth rate on the Si particles is consistent with low growth rates measured for TiN growth on SiO_2 substrates. Under the conditions of our experiment, the activation energy for TiN growth on $Li_4Ti_5O_{12}$ was larger than TiN growth on Si.

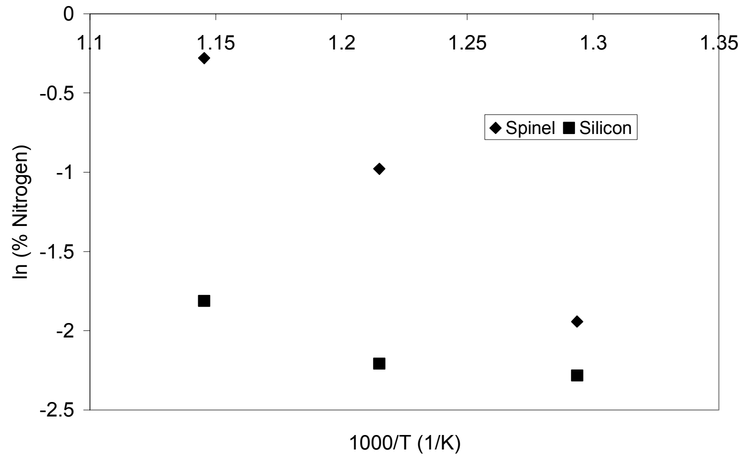

Figure 3: Plot of the natural log of percent nitrogen for Si and $Li_4Ti_5O_{12}$ powders against the inverse temperature (x 1000) of reaction.

Nitrogen content also was plotted against $Li_4Ti_5O_{12}$ and Si powder modified with 100, 250, 500 and 1000 cycles at 600ºC (Figure 4). The slope of the line between 100 and 250 cycles is considerably steeper than the portion between 250 and 1000 cycles for both powders. This difference in slopes shows a transient region at the outset of TiN growth. Extrapolation of the line does not run through the origin indicating that this transient region demonstrates nonlinear growth. Interestingly, the percentage of nitrogen after 100 cycles is roughly only 30% lower than the powder with 250 cycles. Also, the average nitrogen percentage after 500 cycles was slightly greater than the average percentage at 1000 cycles. TiN growth occurs more readily on $Li_4Ti_5O_{12}$ than Si. This is reasonable because the Si surface is naturally oxidized resulting in lower growth rates of TiN as presented above.

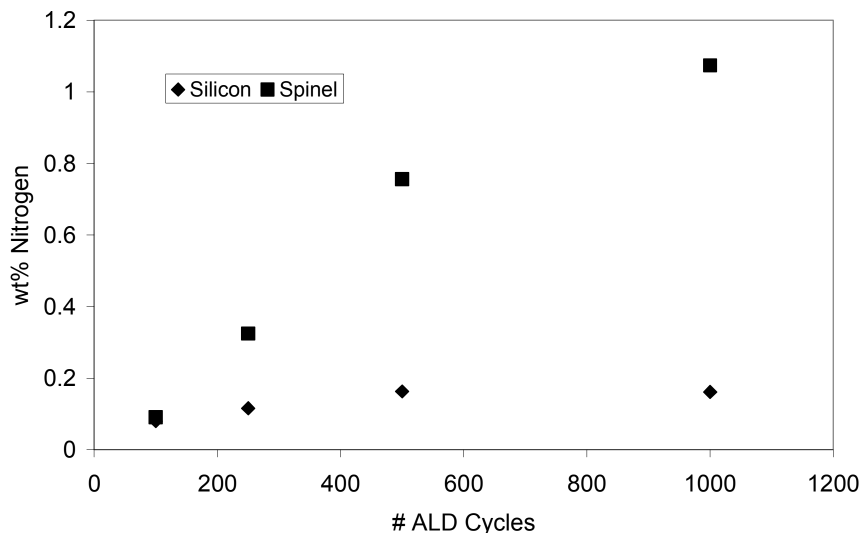

Figure 4: Plot of percent nitrogen content against the number of ALD cycles at 600ºC.

4. Conclusion

The FTIR spectra indicate formation of TiN in the early stage of the reaction on silica while the TEM images show a clear change on the surface of the powder and the potential for coating nanoparticles uniformly. Nitrogen content tests establish the presence of nitrogen on both tested powders. From this collection of data, a TiN thin film has been synthesized on $Li_4Ti_5O_{12}$ and Si powder. However, the mechanism of such a film forming on lithium titanate spinel is undetermined while IR spectral evidence exists for TiN thin film formation on a Si native oxide layer. The growth rate of TiN, as determined from nitrogen content in the coated samples, was significantly higher (up to 10 times) for the lithium titanate spinel powder when compared to the silicon powder. This was expected due to the low growth rates reported for TiN formation on SiO_2 surfaces. The use of these materials in lithium ion batteries is reported in the following section of the report.

References

1. De Baynast, H., A. Bouteville, and J.-C. Remy, *Optimization of titanium nitride rapid thermal CVD process.* Chemical Vapor Deposition, 2000. **6**(3): p. 115-119.
2. Musher, J.N. and R.G. Gordon, *Atmospheric pressure chemical vapor deposition of titanium nitride from tetrakis(diethylamido)titanium and ammonia.* Journal of the Electrochemical Society, 1996. **143**(2): p. 736-44.
3. Mochizuki, Y., et al., *On the reaction scheme for Ti/TiN chemical vapor deposition (CVD) process using TiCl4.* Japanese Journal of Applied Physics, Part 2: Letters, 1995. **34**(3A): p. L326-L329.
4. Ritala, M., et al., *Atomic layer epitaxy growth of TiN thin films.* Journal of the Electrochemical Society, 1995. **142**(8): p. 2731-7.
5. Winter, C.H., et al., *[TiCl4(NH3)2]: An Improved Single-Source Precursor to Titanium Nitride Films. Crystal and Molecular Structure of [TiCl4(TPPO)2] (TPPO = tripiperidinophosphine Oxide.* Inorganic Chemistry, 1994. **33**(6): p. 1227-9.
6. Ishihara, S. and M. Hanabusa, *Laser-assisted chemical vapor deposition of titanium nitride films.* Journal of Applied Physics, 1998. **84**(1): p. 596-599.
7. Min, J.-S., et al., *The mechanism of Si incorporation and the digital control of Si content during the metallorganic atomic layer deposition of Ti-Si-N thin films.* Journal of the Electrochemical Society, 2000. **147**(10): p. 3868-3872.
8. Juppo, M., et al., *Atomic layer deposition of titanium nitride thin films using tert-butylamine and allylamine as reductive nitrogen sources.* Electrochemical and Solid-State Letters, 2002. **5**(1): p. C4-C6.
9. Haukka, S., et al., *Dispersion and distribution of titanium species bound to silica from titanium tetrachloride.* Langmuir, 1993. **9**(12): p. 3497-506.
10. Ritala, M., et al., *Effects of intermediate zinc pulses on properties of TiN and NbN films deposited by atomic layer epitaxy.* Applied Surface Science, 1997. **120**(3/4): p. 199-212.
11. Bellosi, A., E. Landi, and A. Tampieri, *Oxidation behavior of aluminum nitride.* Journal of Materials Research, 1993. **8**(3): p. 565-72.
12. Elam, J.W., et al., *Surface chemistry and film growth during TiN atomic layer deposition using TDMAT and NH3.* Thin Solid Films, 2003. **436**(2): p. 145-156.
13. Kurtz, S.R. and R.G. Gordon, *Chemical vapor deposition of titanium nitride at low temperatures.* Thin Solid Films, 1986. **140**(2): p. 277-90.
14. Fix, R., R.G. Gordon, and D.M. Hoffman, *Low-temperature atmospheric-pressure metal-organic chemical vapor deposition of molybdenum nitride thin films.* Thin Solid Films, 1996. **288**(1-2): p. 116-119.
15. Hausmann, D.M., et al., *Atomic Layer Deposition of Hafnium and Zirconium Oxides Using Metal Amide Precursors.* Chemistry of Materials, 2002. **14**(10): p. 4350-4358.
16. Puurunen, R.L., et al., *Growth of aluminium nitride on porous silica by atomic layer chemical vapour deposition.* Applied Surface Science, 2000. **165**(2-3): p. 193-202.
17. Ferguson, J.D., A.W. Weimer, and S.M. George, *Atomic Layer Deposition of SiO2 Films on BN Particles Using Sequential Surface Reactions.* Chemistry of Materials, 2000. **12**(11): p. 3472-3480.
18. Min, B., et al., *Al2O3 coating of ZnO nanorods by atomic layer deposition.* Journal of Crystal Growth, 2003. **252**(4): p. 565-569.
19. Tripp, C.P. and M.L. Hair, *Reaction of chloromethylsilanes with silica: a low-frequency infrared study.* Langmuir, 1991. **7**(5): p. 923-7.
20. Elers, K.-E., et al., *Diffusion barrier deposition on a copper surface by atomic layer deposition.* Chemical Vapor Deposition, 2002. **8**(4): p. 149-153.
21. Peri, J.B., *Infrared study of OH and NH2 groups on the surface of a dry silica aerogel.* Journal of Physical Chemistry, 1966. **70**(9): p. 2937-45.

22. Gu, W. and C.P. Tripp, *Role of Water in the Atomic Layer Deposition of TiO2 on SiO2.* Langmuir, 2005. **21**(1): p. 211-216.
23. Kim, J., et al., *Properties including step coverage of TiN thin films prepared by atomic layer deposition.* Applied Surface Science, 2003. **210**(3-4): p. 231-239.

Performance of TiN-Coated $Li_4Ti_5O_{12}$ Powder in a Lithium-Ion Battery

1. Introduction

Titanium nitride (TiN) coated nanoparticle powder of $Li_4Ti_5O_{12}$ was tested as a possible anode material for lithium-ion batteries. The nitride was deposited by CVD or ALD methods. The uncoated oxide was also tested for comparison to the coated material.

2. Experimental

The electrodes were prepared by the standard method used by Yardney/Lithion. The electrodes were prepared by coating aluminum or nickel foils with a slurry consisting of 80% $Li_4Ti_5O_{12}$ (active material), 10% SAB (conductive diluent), and 10% PVDF (fluorinated polymer which acts as a binder) in NMP. The slurry was manually coated onto the foils by doctor blade so the thickness of the coating corresponded to 4 – 5 mAh/in² of capacity. After coating, some of the electrodes were calendered. All of the electrodes were dried under vacuum at 110°C. Samples were prepared using both CVD TiN and ALD TiN-coated $Li_4Ti_5O_{12}$.

The electrode materials were tested in coin-type cells. The electrodes were punched to a diameter of 0.51 in². Lithium foil was used as a counter electrode. One-molar solution of $LiPF_6$ in organic carbonate mixed solvent was used as the electrolyte. This electrolyte is typical for lithium-ion cells.

The cells were cycled within 2.1 – 1.2 V. The rate of the first cycle was C/20 (C is the theoretical capacity of the electrode; taking 3 lithium atoms incorporating per formula unit, the specific capacity of the oxide is 175.1 mAh/g). The rate of the following cycles was C/10.

3. Results

Compared to the literature data, the uncoated nanoparticle $Li_4Ti_5O_{12}$ demonstrated similar performance. The capacity was about 145 mAh/g, and the coulombic efficiency was about 99%, which is typical of Li-ion coin cells prepared from other more traditional materials. However, the discharging potential was less stable than in the electrodes where micron-particle size oxide is used. The capacity of the CVD and ALD coated materials were about 20 and 30 mAh/g which is significantly lower than that of the uncoated $Li_4Ti_5O_{12}$. (Since the portion of TiN in the materials was unknown, we included the mass of the TiN as part of active mass for our calculations).

4. Conclusion

Preliminary results from coin cells prepared using nanoparticle $Li_4Ti_5O_{12}$ coated with TiN indicated that these materials could function as reversible anodes in lithium-ion coin cells. The decrease in capacity from the baseline material indicates that further investigation is required to understand the causes for this decrease. There could be several reasons for this. The coating may be too thick. The processing temperature during coating resulted in some agglomeration of nanoparticles resulting in a loss of active surface area. Optimization of the coin cell fabrication to improve coating is also required. For example, varying the size and portion of carbon diluent could improve the inter-particle contact while the variation of the binder fraction may improve the mechanical properties of the electrode.

The synthesis and characterization of TiN layers on nanoparticles via ALD has led to interesting results regarding the formation mechanism, particularly in the early stages of layer formation, which is critical when coating a nanoparticle because ultimately the coating layer should be thin. Our technique involved the sequential deposition of two surface limited half reactions leading to one theoretical monolayer of TiN. The two half reactions were: (A) $TiCl_4$ reacting with the N-H terminated surface and (B) NH_3 reacting with the Ti-Cl terminated surface. Between half-reactions A and B, excess reactant was purged from the system with inert gas. Repeated AB cycling of these half-reactions led to the formation of TiN layers. These sequenced reactions occurring on silica were examined in-situ via FTIR spectroscopy. Ex-situ characterization included Raman spectroscopy, DRIFT IR spectroscopy, X-ray photoelectron spectroscopy and X-ray diffraction.

A reaction mechanism was elucidated for TiN formation from $TiCl_4$ and NH_3 on silica. These results were presented at the 2004 NSF Approaches to Combat Terrorism Workshop and submitted to *Thin Solid Films* as a manuscript. In the initial half-reaction of $TiCl_4$ on silica all hydroxyl modes are reacted. Upon exposure to ammonia, some TiN is formed along with a regeneration of silicon hydroxyls, as observed by FTIR. As layers progress, some TiN is oxidized to TiO_2 also. As a result, there are two separate competitive reactions going on: (i) TiN formation and silica regeneration and (ii) TiN formation and TiO_2 formation. It is assumed that the presence of small amounts of water vapor contribute to both competitions, particularly the second one. It is not clear yet what role ammonia plays in the first competition. It takes approximately 50-100 reaction cycles to achieve a stable TiN layer as observed by Raman spectroscopy. This corresponds to an approximate layer thickness of 30Å (based on literature values).

Thin films of TiN were formed on both $Li_4Ti_5O_{12}$ and Si nanoparticles. The reaction rates for TiN on these materials were considerably higher than on silica due to the differences in surface chemistry. A series of depositions were performed varying cycle time and growth temperature. The coatings were analyzed for nitrogen content and morphology using analytical techniques. Coated $Li_4Ti_5O_{12}$ samples were used to fabricate coin cells at Yardney Technical Products, Inc./Lithion, Inc. and compared to non-coated $Li_4Ti_5O_{12}$ samples. A reduction in capacity for the coin cells from 145 to 30 mAh/g was measured for the TiN-coated anodes. It was concluded that the TiN-coated samples could work as a reversible anode in a lithium-ion coin cell, however further optimization of the coating process as well as the battery fabrication methods need to be examined to draw firmer conclusions.